Published in final edited form as:

Inorg Chem. 2017 February 20; 56(4): 2233–2240. doi:10.1021/acs.inorgchem.6b02899.

Photoinduced Reductive Elimination of H_2 from the Nitrogenase Dihydride (Janus) State Involves a FeMo-cofactor-H_2 Intermediate

Dmitriy Lukoyanov[†], **Nimesh Khadka**[§], **Dennis R. Dean**[#], **Simone Raugei**[‡], **Lance C. Seefeldt**[§,*], and **Brian M. Hoffman**[†,*]

[†]Department of Chemistry, Northwestern University, Evanston, IL 60208

[§]Department of Chemistry and Biochemistry, Utah State University, Logan, UT 84322

[#]Department of Biochemistry, Virginia Tech, 110 Fralin Hall, Blacksburg, VA 24061

[‡]Pacific Northwestern National Laboratory, Richland, Washington 99352, United States

Abstract

N_2 reduction by nitrogenase involves the accumulation of four reducing equivalents at the active site FeMo-cofactor to form a state with two [Fe-H-Fe] bridging hydrides (denoted $E_4(4H)$, the Janus intermediate), and we recently demonstrated that the enzyme is activated to cleave the N≡N triple bond by the reductive elimination (*re*) of H_2 from this state. We are exploring a photochemical approach to obtaining atomic-level details of the *re* activation process. We have shown that when $E_4(4H)$ at cryogenic temperatures is subjected to 450 nm irradiation in an EPR cavity, it cleanly undergoes photoinduced *re* of H_2 to give a reactive doubly-reduced intermediate, denoted $E_4(2H)$*, which corresponds to the intermediate that would form if thermal dissociative *re* loss of H_2 preceded N_2 binding. Experiments reported here establish that photoinduced *re* occurs in two steps. Photolysis of $E_4(4H)$ generates an intermediate state that undergoes subsequent photoinduced conversion to [$E_4(2H)$* + H_2]. The experiments, supported by DFT calculation, indicate that the trapped intermediate is an H_2 complex on the ground adiabatic potential energy suface that connects $E_4(4H)$ with [$E_4(2H)$* + H_2]. We suggest this complex, denoted $E_4(H_2; 2H)$, is a thermally populated intermediate in the catalytically central *re* of H_2 by $E_4(4H)$, and that N_2 reacts with this complex to complete the activated conversion of [$E_4(4H)$ + N_2] into [$E_4(2N2H)$ + H_2].

TOC image

Corresponding author: bmh@northwestern.edu; lance.seefeldt@usu.edu.

Supporting Information Available: Kinetics data; EPR decomposition protocol; discussion of energy landscapes; details of DFT calculations; 5 figures in all.

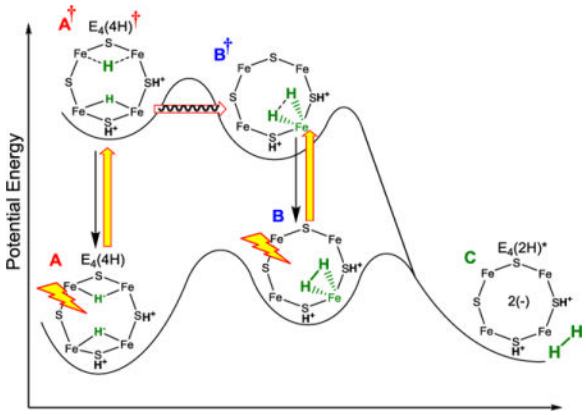

Introduction

In recent years we have demonstrated[1–4] that N_2 reduction by nitrogenase involves the accumulation of four reducing equivalents at the active site FeMo-cofactor (FeMo-co) to form a state with two [Fe-H-Fe] bridging hydrides and two sulfur-bound protons (denoted $E_4(4H)$, the Janus intermediate), and that breaking the N≡N triple bond requires the reductive elimination (*re*) of H_2 from $E_4(4H)$. This process corresponds to the forward direction of the equilibrium in Fig 1, **upper**, whose reverse is the oxidative addition (*oa*) of H_2 with release of N_2.[5] This *re/oa* mechanism was initially founded on the identification of a freeze-trapped intermediate of the α-$70^{Val\rightarrow Ile}$ substituted MoFe protein as $E_4(4H)$.[6–8] Subsequently, EPR/ENDOR, and photophysical measurements showed that the identical Janus intermediate can be freeze-trapped during N_2 reduction by wild type (WT) MoFe protein, thereby confirming the intermediate in the α-$70^{Val\rightarrow Ile}$ variant as a reliable guide to mechanism, and establishing *re/oa* as a thermoneutral, kinetically accessible equilibrium process.[4] The overall result of these several findings was to establish that H_2 release drives the reduction of the N≡N triple bond, and thus the mechanistic requirement for the formation of one H_2 per N_2. This in turn implies the limiting stoichiometry of eight electrons/protons for the reduction of N_2 to two NH_3 (eq 1).[3]

$$N_2+8e^-+16ATP+8H^+ \rightarrow 2NH_3+H_2+16ADP+16P_i \quad (1)$$

In the context of this stoichiometry, and the Lowe-Thorneley kinetic scheme that embodies it,[9–11] one sees that $E_4(4H)$ sits at a transition in the N_2 reduction pathway, poised to relax to E_0 through sequential release of two H_2, but equally poised to bind and reduce N_2 through the accumulation of four more equivalents, hence the designation of $E_4(4H)$ as the Janus intermediate.[2]

As a part of our efforts to *(i)* more deeply integrate the *re/oa* mechanism into the organometallic chemistry of hydrides and *(ii)* obtain atomic-level details of the *re* activation process we adopted a photochemical approach inspired by the properties of inorganic dihydride complexes.[12] The photolysis of transition metal dihydride complexes, primarily mononuclear centers with *cis* hydride ligands, commonly results in the release of H_2[13–22]

with a decrease in metal-ion oxidation state by two, “a typical example of reductive elimination”, while the thermally induced reverse reaction “is the prototype example of an oxidative addition reaction.”[14] EPR and ENDOR measurements showed that when the nitrogenase $E_4(4H)$ intermediate is subjected to 450 nm irradiation in an EPR cavity, it cleanly undergoes photo-induced *re* of H_2 to give an intermediate which we denote $E_4(2H)$*, Figure 1, **lower**. It is a reactive version of the $E_2(2H)$ state that has accumulated two [e^-/H^+], and corresponds to the intermediate that would form upon thermal dissociative *re* loss of H_2 prior to N_2 binding. The photoinduced *re* of H_2/D_2 from $E_4(4H)/E_4(4D)$ in H_2O/D_2O is temperature invariant in *both* buffers in the range of 4 – 12 K, a variation in the thermal energy (proportional to T) by a factor of ~ 3, and the photoinduced decay of Janus intermediate shows a large KIE over this range, defined as the ratio of the median decay times for D_2O and H_2O buffers: KIE ~ 10. These observations together imply that photoinduced release of H_2 through *re* involves nuclear tunneling through a barrier, in contrast to the barrierless process inferred for mono-metallic metal complexes.[14,18]

The photoinduced state $E_4(2H)$* relaxes to $E_4(4H)$ by the thermally activated *oa* of H_2 to $E_4(2H)$* (Figure 1, **lower**) during annealing of the frozen solid at temperatures above $T \gtrsim 175$ K. The observation of a significant KIE plus a strong temperature dependence in the *oa* process revealed that it involves traversal of an energy barrier associated with H_2 binding and/or bond cleavage. Overall, the measurements led to proposed energy surfaces associated with photoinduced *re/oa* for the Janus intermediate that will be refined in the present report.

The reported results were consistent with the absence of intermediate state(s) during photoinduced *re*,[23] but they left open that possibility. As we noted: “whether the process involves an actual intermediate H_2 complex remains to be determined”. Experiments reported here not only establish the presence of an intermediate in the photoinduced *re* of H_2, but furthermore show that this intermediate undergoes photoinduced *re* to $E_4(2H)$* (Fig 1, **lower**). The experiments, supported by DFT calculation, indicate that the trapped intermediate is an H_2 complex and lead us to suggest that it functions as an intermediate in the thermal *re* of H_2 that activates FeMo-co to break the N≡N triple bond.

Materials and Methods

Materials and Protein purifications

All the reagents were obtained from SigmaAldrich (St. Louis, MO) or Fisher Scientific (Fair Lawn, NJ) and were used without further purification. Argon and N_2 were purchased from Air Liquide America Specialty Gases LLC (Plumsteadville, PA).

Remodeling the active site of MoFe protein by the α-$70^{Val\rightarrow Ile}$ mutation permits the freeze trapping of MoFe with high populations of $E_4(4H)$[6] identical to that in WT enzyme.[4] The protein was obtained from the corresponding *Azotobacter vinelandii* strains as described elsewhere.[24] The handling of all buffers and proteins were done anaerobically under Ar atmosphere or under Schlenk vacuum line unless stated otherwise.

EPR samples

The E_4(4H) intermediate and its deuterated analogue, E_4(4D), are prepared by turnover of the MoFe protein in H_2O and D_2O buffers, respectively. EPR samples were prepared in a dioxygen free buffer and freeze-trapped during turnover as described.[12]

EPR Measurements

X-band EPR spectra were recorded on a Bruker ESP 300 spectrometer equipped with an Oxford Instruments ESR 900 continuous He flow cryostat. All spectra were measured at the following conditions: temperature, 12 K; microwave frequency, 9.36 GHz; microwave power, 10 mW; modulation amplitude, 9 G; time constant, 160 ms; field sweep speed, 20 G/s. *In situ* photolysis of a sample held within the cryostat employed a Thorlabs Inc (Newton, New Jersey) PL450B, 450 nm, 80 mW Osram Laser Diode mounted on the cavity optical access port as described.[12] Light intensity was varied through controlling the laser current.[25] Data points for observed photolysis progress curves were obtained as well resolved g_1 amplitudes of corresponding EPR signals, with normalization of total concentration of the intermediate species to unity.

Results and Discussion

EPR Spectra and Low-temperature Photoinduced re

As recently shown,[12] *intra cavity* photolysis with 450 nm light of the $S = ½$ E_4(4H) intermediate freeze-trapped during turnover of MoFe protein causes photoinduced conversion of the E_4(4H) signal, **g** = [2.15, 2.007, 1.965], to the E_4(2H)* signal with **g** = [2.098, 2.0, 1.956], and E_4(2H)* completely relaxes back to E_4(4H) by *oa* of H_2 with annealing in the solid state at temperatures above ~ 175 K.

To simultaneously obtain the time course for both the photoinduced loss of the E_4(4H) (**A**) and the appearance of the E_4(2H)* (**C**) signals, rather than continuously monitoring the occupancy of E_4(4H) during photolysis, we collected complete spectra at multiple times during 12 K and 50 K irradiation and measured the intensities of the two species as a function of time, Fig 2. If photoexcitation of **A** led directly to the **A** (E_4(4H)) → **C** (E_4(2H)*) conversion in a single kinetic step without buildup of a spectroscopic intermediate state, then at every time the **C** occupancy should equal the loss of the **A** occupancy, (1-**A**) as normalized to the value **A** at $t = 0$, and the rate parameters for the rise of **C** should equal those for the loss of **A**. However, as shown in Fig 2 (and see below), at low temperatures the rise of **C** lags the loss of **A**, which implies that photoexcitation of **A** creates an intermediate, **B**, which accumulates during the course of its conversion to **C.** The existence of such an on-path state **B**, is supported below in the characterization of **B**, kinetic fits, and in considerations of a potential-energy surfaces that captures the reversible [photoinduced-*re*/thermal-*oa*] process of Fig 1 **lower**.

Photolysis Intermediate—To observe the **B** intermediate directly we carried out a variant of the photolysis cryoannealing experiment. E_4(4H) was photolyzed for a fixed interval (25 min) at successively higher temperatures, then cooled back to 12 K for examination. In each step the sample was then annealed at 77 K for 2 min then restored to

12 K for another round of EPR examination. After such a process following photolysis at a given temperature, the sample was annealed at ~ 215 K, at which temperature E_4(2H)* relaxes to E_4(4H) within 2 minutes, thus restoring the sample to its initial state for photolysis at the next temperature (Fig 3).

Consider the results for this annealing process as applied to the samples photolyzed at 12 K (Figs 3, 4). Photolysis has converted the majority of E_4(4H) to E_4(2H)*, which does not relax during 77 K annealing. However, this annealing causes a small recovery of the E_4(4H) signal without increase in the E_4(2H)* signal. This implies another state, **B**, has been formed by photolysis, that **B** is stable in the dark at temperatures, $T \lesssim 30$ K, and that it relaxes to E_4(4H) by 77 K, even though E_4(2H)* does not relax at this temperature. Essentially the same recovery of E_4(4H) upon annealing is observed with 20 K photolysis, but by photolysis at 30 K, the recovery upon 77 K annealing is clearly diminished, implying a lesser accumulation of **B**. When photolysis is carried out above 30 K, there is no recovery of E_4(4H) with 77 K annealing, indicating that **B** does relax at 30 K and above.

The measurements in Figs 3 showed the way to acquiring the spectrum of **B** through subtraction. The use of three spectra – before irradiation, after irradiation, after 77 K annealing – allows a subtraction-elimination of signals from all species except **B**. The procedure is shown in Fig S1, and as can be seen in Fig 4, reveals an $S = ½$ signal for **B** with **g** ~ [2.02, 2.00, 1.97]. Despite the need for this cumbersome subtraction procedure, the time course of **B** could actually be followed during photolysis at 12 K, as well as those of the initial **A** = E_4(4H) and final **C** = E_4(2H)* states to which it is kinetically linked by the kinetic scheme of eq 2.

The finding that **B** persists indefinitely (hours) at low temperature (T < 30 K) in the absence of the actinic light, yet converts to **C** during photolysis at these temperatures implies that both the **A**→ **B** and **B** → **C** conversions are photoinduced: the photoconversion of **A** to **C** thus involves two steps, each of which requires the absorption of a photon, as incorporated in the scheme of eq 2:

$$\mathbf{A} \xrightarrow{h\nu} \mathbf{B} \xrightarrow{h\nu} \mathbf{C} \quad (2)$$

Though surprising, this result nonetheless can be analogized to the textbook photocleavage of a methyl C-H bond during photolysis of toluene, which likewise requires two consecutive photons.[26–28]

This finding does, however, require that we revisit our initial assignment of the photolysis product **C** = E_4(2H)*, Fig 1, **lower.** In that earlier report, in addition to *re* mechanism of photoinduced *re* of H_2 to yield **C** = E_4(2H)*, now shown to be a 2-step process, eq 2, Fig 5, **upper**, we considered two other 2-step mechanisms that might eliminate the hydride bridges of E_4(4H), each mechanism having a different assignment of the photoproduct, **C**, Fig 5.

One of those alternative interpretations postulates two steps of photoinduced hydride protonolysis (*hp*; Fig 5, **middle**), each with loss of H_2. This mechanism can be dismissed,

for it would not lead to a photoproduct **C** that can regenerate $E_4(4H)$ during cryoannealing, as observed. Instead it would lead to FeMo-co at the E_0 resting state level, which could not react with two released H_2 to regenerate $E_4(4H)$ during cryoannealing: neither E_0 nor $E_2(2H)$ react with H_2.[29]

The second alternative shown in Fig 5, **lower** posits two steps of photoinduced *re* of a single hydride, each with transfer of the proton 'released' to a bridging sulfide. Instead of resulting in the release of H_2, the final result of such a process would be creation of an $E_4(4H)$ 'isomer' with four protonated sulfur and no hydrides. Simple considerations of the expected relative stabilities of the experimentally observed **B** and **C** states rule out this mechanism. **B** is dark-stable at low temperatures and reverts to $E_4(4H)$ at T > 30 K, while **C** is more stable than **B**, relaxing to **A** only at T > 175 K. The greater stability of **C** is understandable within the *re* mechanism. The product state, **C** = $E_4(2H)$*, undergoes activated 'second-order' binding of H_2 on the ground potential-energy surface in the frozen matrix, to **B** as a higher-energy intermediate, which undergoes *oa* of H_2 to generate the bridging hydrides of **A** = $E_4(4H)$. In contrast, in the *L* mechanism **B** is the destabilized $E_4(L_1)$ 'isomer' of $E_4(4H)$ (Fig 5), and **C** would be a yet more unstable $E_4(L_2)$ isomer. But this would be expected to relax to $E_4(L_1)$ at a temperature *lower* than T ~ 30 K where **B** reverts to **A**, not at a temperature ~145 K *higher*.

These qualitative ideas are supported by exploratory DFT calculations (SI) on a realistic model of E_4 and its local environment (Fig S4), which show that any structure with more than two protonated sulfur atoms is very high in energy relative to $E_4(2H)$* and other relevant E_4-level states, with $E_4(L_2)$ much higher in energy than $E_4(L_1)$ (Fig S5). Thus, the greater stability of **C** than **B** is indeed incompatible with the *L* mechanism.

Potential-Energy Landscape

The above results can be captured by several alternative heuristic potential-energy landscapes. The most attractive of such qualitative conceptualizations is shown in Fig 6, which represents a projection of multi-dimensional potential energy surfaces that incorporate the experimental observations, along with features of *re/oa* of H_2 associated with conventional inorganic complexes.

The low-temperature steady-state photoinduced **A** → **C** *re* of H_2 on the landscape of Fig 6 is visualized as following a pathway in which photoexcitation of **A** produces $\mathbf{A}^{\dagger}$, which tunnels through a barrier to form an excited H_2 complex, $\mathbf{B}^{\dagger}$, which undergoes rapid relaxation to the observed $S = ½$, intermediate **B** on the ground surface. The **B** → **C** conversion then occurs by photoexcitation of **B** to $\mathbf{B}^{\dagger}$, which undergoes tunneling/barrier crossing on its way to the *re* of H_2 in state **C**; in the absence of direct evidence for nuclear tunneling by $\mathbf{B}^{\dagger}$, tunneling is not indicated.

Although we as yet have no direct evidence as to the structure of the observed **B** intermediate (Fig 4), as visualized in Fig 6 the behavior of inorganic H_2 complexes[30–32] indicates that this intermediate is an H_2-bound state on the ground adiabatic potential-energy surface, a possibility first noted thirty years ago.[33] Firstly, thermally induced *re/oa* of inorganic H_2 complexes generally proceed through such an intermediate,[23] indicating an

expectation that such a state is present on the ground adiabatic surface as shown in Fig 6. Secondly, the assignment of **B** as such a complex is supported by the finding that the **B** → **C** *re* of H_2 is photoinduced: such behavior has been established for inorganic-H_2 complexes.[13,34–37] In support of this assignment, the DFT calculations (Fig S5 suggest that **A** = E_4(4H) and **C** = E_4(2H)* (+ H_2) are the most stable E_4 states and are very close in energy, and that they likely are connected by **B** = E_4(H_2; 2H) at a slightly higher energy.

As a final note, in SI support is provided for the assignment of **B** as on-path. There we show that an alternative assignment of the observed $S = ½$ intermediate, Figs 3, 4, to an off-path state, **D**, Fig S3 is inconsistent with experiment. It is shown that in general, if an off-path intermediate that both forms and decays photochemically were to be observed, then it would have to steadily accumulate during low-temperature photolysis, rather than approach a steady-state population as seen in detailed kinetic measurements presented below.

Kinetic Scheme

In the context of the landscape of Fig 6, the finding that the photoconversion of **A** to **C** involves the dark-stable intermediate **B** and the absorption of two photons consecutively, with **B** reverting solely to **A** for T > 30 K, implies the minimum kinetics of Scheme 1. During steady-state photoexcitation of **A** = E_4(4H), one photon forms the excited state, $\mathbf{A}^\dagger$ = $E_4(4H)^\dagger$. This can decay back to **A** or tunnel through the energy barrier to form $\mathbf{B}^\dagger$, without return at low temperature ($k_b \approx 0$). This excited state branches: it can proceed directly with the *re* of H_2 to form **C**, but, primarily decays to **B** ($k_d' > k_{B\dagger C}$). **B** is dark-stable at low temperatures ($k_{BA} \approx 0$), so would accumulate, but reaches a steady-state population because photoexcitation of **B** re-forms $\mathbf{B}^\dagger$, and cycling through this process ultimately allows **A** to convert entirely to **C** during prolonged steady-state photolysis. At higher temperatures, T ≳ 30 K, **B** is no longer dark-stable, which implies that the $\mathbf{A}^\dagger \rightleftharpoons \mathbf{B}^\dagger$ reaction becomes reversible and/or direct reversion of **B** to **A** becomes operative: [k_b and/or k_{BA}] > 0. At temperatures, below ~ 175 K, **C** is indefinitely stable, $k_{CB} \approx 0$. Upon warming the frozen solid to T ≳ 175 K, **C** relaxes to **A**, [k_{CB}, k_{BA}] > 0, namely E_4(2H)* undergoes *oa* of H_2 to regenerate E_4(4H), passing through the H_2 intermediate **B** on the ground adiabatic surface of Fig 6.

Considering in more detail the predictions of Scheme 1 in the steady-state photolysis measurements for temperatures T < 175 K, where **C** accumulates ($k_{CB} \approx 0$), the rate constant for formation of the photoexcited $\mathbf{A}^\dagger$ state is the product of the temperature-independent quantum yield, ϕ_A (taken to include the extinction coefficient) with the light intensity, I_0, and k_d is the rate constant for direct relaxation of $\mathbf{A}^\dagger$ back to ground. It can be presumed that k_d is by far the largest rate constant in this scheme, and as a result, $\mathbf{A}^\dagger$ will enter a photostationary state during the *intra-cavity* photolysis, with instantaneous population proportional to the instantaneous concentration of **A**, with a temperature-independent proportionality constant determined by the photophysical constants,

$$A^\dagger = \frac{\phi_A I_o}{k_d} A \quad (3)$$

and analogously for $\mathbf{B}^{\dagger}$. As a result, Scheme 1 maps onto the far-simpler Scheme 2, an elaboration of eq 2, with a two photoinduced reaction steps involving observable states, but with provision for the first step to become reversible at higher temperatures. The net rate constant for the **A** → **B** conversion in Scheme 2 is given by

$$k_1 = \frac{\phi_A I_o}{k_d} k_A^{\dagger} \quad (4)$$

where $k_{A\dagger}$ is the (tunneling) rate constant for $\mathbf{A}^{\dagger} \rightarrow \mathbf{B}^{\dagger}$ conversion. The rate constant for the second step, k_2, takes an analogous form; we show shortly that this is augmented by an activated, thermally induced contribution.

Kinetic Measurements

Progress curves for photolysis at 12 K and 50 K were collected for the frozen sample in H_2O buffer, Fig 7, and D_2O buffer, Fig S2. A fit to Scheme 2 using stretched exponentials, a decay function written, $\exp(-(t/\tau)^m)$, with median time constant, τ and 'stretch parameter', $0 < m \leq 1$, which decreases with deviations from simple exponential ($m = 1$). This description is needed to incorporate variation in I_0 over the sample tube caused by light-scattering by the 'frozen snow' samples,[12] and yields rate parameters listed on Fig 7. As shown in this figure, at 12 K the occupancy of **B** quickly rises to a value of roughly 20% occupancy that persists over the time of the experiment. Within the errors of determining the occupancy of intermediate **B** by the subtraction procedure described above, and of using stretched exponentials to model the distribution in apparent rate constants caused by light scattering, the measured time course of **B** at 12 K is in satisfactory agreement with the time course predicted by an 'omit-fit', namely a fit of the progress curves of **A** and **C** alone to eq 2, the low-temperature limit of the more elaborate Scheme 2.

In discussing the stretched-exponential rate parameters that describe the progress curves in Fig 7, there are different possible ways to define the correspondence of a rate constant defined in Scheme 2 with the stretched-exponential time-constant τ and 'stretch parameter, $0 < m \leq 1$[38] For present purposes it is adequate to discuss the results as though rate constant and time constant are inverses: $k \sim 1/\tau$.

Considering the 12 K measurements, **B** is stable at this temperature, which implies that at this temperature the rate constants for $\mathbf{B}^{\dagger} \rightarrow \mathbf{A}^{\dagger}$ and direct **B** → **A** reversion are vanishingly small, $k_{-1} \sim 0$. As a result, the photoinduced decay of **A** as measured by steady-state *intracavity* photolysis corresponds directly to k_1 (eq 4). The fit to the present measurements at 12 K shown in Fig 7 confirm the previously reported low-temperature kinetic parameters for the **A** → **B** as well as the large isotope effect associated with k_1, KIE ~ 13 (Fig S2). It was shown in the earlier measurements from 3.8 – 12 K that this process exhibits $\mathbf{A}^{\dagger} \rightarrow \mathbf{B}$ tunneling associated with the factor, $k_{A\dagger}$, that is incorporated into k_1 (eq 4). Importantly, experiments in which the intensity of the actinic light is varied we find that k_1 exhibits the expected linear dependence, eq 4. In the fits to Scheme 2 the time constant for **A** → **B** is unchanged by warming from 12 → 50 K (Fig 7), consistent with a persistence of the $\mathbf{A}^{\dagger} \rightarrow \mathbf{B}$ tunneling and continuation of the temperature invariance of the tunneling rate constant

previously seen between 4 and 12K.[12] However, the overall reversion of **B** to **A** (k_{-1}) has become significant by 50 K.

The rate constant, k_2, for the photoinduced **B** → **C** conversion is much greater than k_1 at 12 and 50 K (Fig 7). As with k_1, at 12 K it exhibits the expected linear dependence on actinic light intensity and a large isotope effect, KIE ≳ 10. The significant KIE plus an observed increase with increasing temperature dependence (Fig 7) is consistent with the $\mathbf{B}^{\dagger}$ → **C** with loss of H_2 involving traversal of or tunneling through an energy barrier, rather than excitation of **B** to a dissociative state.

On the Structure of $A^{\dagger}$, and the mechanism of $A^{\dagger}$→B conversion

Regarding the nature of the excited state $\mathbf{A}^{\dagger}$, as previously,[12] we suggest that photoinduced *re* is initiated by excitation of E_4(4H) into a (σ*) antibonding ligand-field excited state of one of the two bridging hydrides, as in the orbital sketch of Fig 8, which leads to the cartoon representation of $\mathbf{A}^{\dagger}$ in Fig 6. We suggest that this anti-bonding state could undergo reductive elimination, liberating a proton that tunnels the short distance to the second hydride bridge and protonates that hydride, thereby generating the intermediate $\mathbf{B}^{\dagger}$, the excited state of H_2-bound FeMo-co (**B**).

Conclusions

This report describes a detailed study of the photoinduced *re* of H_2 by E_4(4H) to form the activated E_4(2H)* state, and the thermal regeneration of E_4(4H) by the *oa* of H_2 to E_4(2H)*, Fig 1, **lower**. We have examined the progress curves for loss of E_4(4H) and appearance of E_4(2H)* at 12 K and 50 K with samples prepared in H_2O and D_2O buffer. The key advance of these measurements is the discovery and characterization of a photogenerated intermediate, **B**, whose properties assign it as an H_2 complex on the pathway for thermal *oa* of H_2 by E_4(2H)*, as visualized in Fig 6. This state accumulates during 12 K photolysis, and is dark-stable at this temperature, but can undergo photoinduced *re* to release H_2.

The present study furthers our effort to obtain atomic-level details of the central mechanistic step in nitrogen fixation, *re* of H_2 by E_4(4H) coupled to the binding/reduction of N_2, by which the nitrogenase MoFe protein is activated to carry out one of the most challenging chemical transformation in biology, the reduction of the N≡N triple bond. In the present work we extend the use of a photochemical approach inspired by the photoinduced *re* of H_2 by inorganic dihydride complexes. Our initial report showed that E_4(4H) exhibits the photoinduced *re/oa* equilibrium of Fig 1,[12] and we subsequently showed that the E_4(4H) in the α-$70^{Val\rightarrow Ile}$ variant and the WT enzyme are identical in properties and behavior.[4]

The initial study of E_4(4H) photolysis[12] did not detect an intermediate state during photoinduced *re* of H_2 from E_4(4H). However, the more detailed experiments reported here now establish the presence of an intermediate, and furthermore show that this photogenerated intermediate can proceed to form E_4(2H)* through subsequent photoinduced *re* with loss of H_2. These findings, supported by DFT calculations, lead us to conclude that the trapped intermediate is an H_2 complex on the ground adiabatic potential energy suface that connects E_4(4H) with [E_4(2H)* + H_2], Fig 6. As such, we further suggest that this H_2

complex is a thermally populated intermediate in the catalytically central *re* of H_2 by $E_4(4H)$, and that N_2 reacts with this complex to complete the conversion of [$E_4(4H)$ + N_2] into [$E_4(2N2H)$ + H_2], Fig 9. Whether there are additional intermediates in this catalytic conversion remains to be determined. We do not at this point favor the idea that $E_4(2H)$* itself is such an intermediate. If H_2 were thermally released from FeMo-co before N_2 binds, forming $E_4(2H)$*, then it is hard to see why D_2 would *not* undergo *oa* by this FeMo-co state, contrary to the observation that D_2 does not react with MoFe protein during turnover in the absence of N_2.[9]

Supplementary Material

Refer to Web version on PubMed Central for supplementary material.

Acknowledgments

This work was supported by the NIH (GM 111097; BMH), NSF (MCB 1515981 to BMH) and U.S. Department of Energy, Office of Science, Basic Energy Sciences (BES) (DESC0010687 and DE-SC0010834; LCS and DRD), and the Division of Chemical Sciences, Geosciences, and Bio-Sciences (S.R.).

References

1. Hoffman BM, Lukoyanov D, Yang ZY, Dean DR, Seefeldt LC. Mechanism of Nitrogen Fixation by Nitrogenase: The Next Stage. Chem Rev. 2014; 114:4041–4062. [PubMed: 24467365]
2. Hoffman BM, Lukoyanov D, Dean DR, Seefeldt LC. Nitrogenase: A Draft Mechanism. Acc Chem Res. 2013; 46:587–595. [PubMed: 23289741]
3. Lukoyanov D, Yang ZY, Khadka N, Dean DR, Seefeldt LC, Hoffman BM. Identification of a Key Catalytic Intermediate Demonstrates That Nitrogenase Is Activated by the Reversible Exchange of N_2 for H_2. J Am Chem Soc. 2015; 137:3610–3615. [PubMed: 25741750]
4. Lukoyanov D, Khadka N, Yang ZY, Dean DR, Seefeldt LC, Hoffman BM. Reductive Elimination of H_2 activates Nitrogenase to Reduce the N≡N Triple Bond: Characterization of the $E_4(4H)$ Janus Intermediate in Wild-Type Enzyme. J Am Chem Soc. 2016; 138:10674–10683. [PubMed: 27529724]
5. A knowledgeable reviewer noted that a more common notation uses capitals in the abbreviations (RE, OA), but we feel that it is beneficial to retain consistency with our earlier reports.
6. Igarashi RY, Laryukhin M, Dos Santos PC, Lee HI, Dean DR, Seefeldt LC, Hoffman BM. Trapping H- Bound to the Nitrogenase FeMo-Cofactor Active Site During H2 Evolution: Characterization by Endor Spectroscopy. J Am Chem Soc. 2005; 127:6231–6241. [PubMed: 15853328]
7. Lukoyanov D, Yang Z-Y, Dean DR, Seefeldt LC, Hoffman BM. Is Mo Involved in Hydride Binding by the Four-Electron Reduced (E_4) Intermediate of the Nitrogenase MoFe Protein? J Am Chem Soc. 2010; 132:2526–2527. [PubMed: 20121157]
8. Lukoyanov D, Barney BM, Dean DR, Seefeldt LC, Hoffman BM. Connecting Nitrogenase Intermediates with the Kinetic Scheme for N_2 Reduction by a Relaxation Protocol and Identification of the N2 Binding State. PNAS. 2007; 104:1451–1455. [PubMed: 17251348]
9. Burgess BK, Lowe DJ. Mechanism of Molybdenum Nitrogenase. Chem Rev. 1996; 96:2983–3012. [PubMed: 11848849]
10. Thorneley RNF, Lowe DJ. Kinetics and Mechanism of the Nitrogenase Enzyme System. Metal Ions in Biology. 1985; 7:221–284.
11. Wilson PE, Nyborg AC, Watt GD. Duplication and Extension of the Thorneley and Lowe Kinetic Model for *Klebsiella Pneumoniae* Nitrogenase Catalysis Using a Mathematica Software Platform. Biophysical Chemistry. 2001; 91:281–304. [PubMed: 11551440]

12. Lukoyanov D, Khadka N, Yang ZY, Dean DR, Seefeldt LC, Hoffman BM. Reversible Photoinduced Reductive Elimination of H2 from the Nitrogenase Dihydride State, the E_4(4H) Janus Intermediate. J Am Chem Soc. 2016; 138:1320–1327. [PubMed: 26788586]
13. Perutz RN, Procacci B. Photochemistry of Transition Metal Hydrides. Chem Rev. 2016
14. Perutz RN. Metal Dihydride Complexes: Photochemical Mechanisms for Reductive Elimination. Pure and Applied Chemistry. 1998; 70:2211–2220.
15. Colombo M, George MW, Moore JN, Pattison DI, Perutz RN, Virrels IG, Ye TQ. Ultrafast Reductive Elimination of Hydrogen from a Metal Carbonyl Dihydride Complex; a Study by Time-Resolved IR and Visible Spectroscopy. Journal of the Chemical Society-Dalton Transactions. 1997:2857–2859.
16. Whittlesey MK, Mawby RJ, Osman R, Perutz RN, Field LD, Wilkinson MP, George MW. Transient and Matrix Photochemistry of $Fe(Dmpe)_2H_2$ (Dmpe = $Me_2PCH_2CH_2PMe_2$) - Dynamics of C-H and H-H Activation. J Am Chem Soc. 1993; 115:8627–8637.
17. Ballmann J, Munha RF, Fryzuk MD. The Hydride Route to the Preparation of Dinitrogen Complexes. Chem Commun. 2010; 46:1013–1025.
18. Ozin GA, Mccaffrey JG. The Photoreversible Oxidative-Addition, Reductive-Elimination Reactions Fe+H_2-Reversible-FeH_2 in Low-Temperature Matrices. J Phys Chem. 1984; 88:645–648.
19. Dugan TR, Holland PL. New Routes to Low-Coordinate Iron Hydride Complexes: The Binuclear Oxidative Addition of H_2. J Organomet Chem. 2009; 694:2825–2830.
20. Yu Y, Smith JM, Flaschenriem CJ, Holland PL. Binding Affinity of Alkynes and Alkenes to Low-Coordinate Iron. Inorg Chem. 2006; 45:5742–5751. [PubMed: 16841977]
21. Smith JM, Sadique AR, Cundari TR, Rodgers KR, Lukat-Rodgers G, Lachicotte RJ, Flaschenriem CJ, Vela J, Holland PL. Studies of Low-Coordinate Iron Dinitrogen Complexes. J Am Chem Soc. 2006; 128:756–769. [PubMed: 16417365]
22. Yu Y, Sadique AR, Smith JM, Dugan TR, Cowley RE, Brennessel WW, Flaschenriem CJ, Bill E, Cundari TR, Holland PL. The Reactivity Patterns of Low-Coordinate Iron-Hydride Complexes. J Am Chem Soc. 2008; 130:6624–6638. [PubMed: 18444648]
23. Mas-Balleste, R., Lledos, A. From Dihydrogen to Dihydride: Homolytic Splitting of H_2. In: Alvarez, S., editor. Comprehensive Inorganic Chemistry Ii. Vol. 9. Elsevier Ltd; 2013. p. 736-740.
24. Christiansen J, Goodwin PJ, Lanzilotta WN, Seefeldt LC, Dean DR. Catalytic and Biophysical Properties of a Nitrogenase Apo-MoFe Protein Produced by a NifB-Deletion Mutant of *Azotobacter Vinelandii*. Biochemistry. 1998; 37:12611–12623. [PubMed: 9730834]
25. https://www.thorlabs.com/thorproduct.cfm?partnumber=PL450B, see MFG Spec pdf file, page 4.
26. Michl, J., Bonacic-Koutecky, V. Electronic Aspects of Organic Photochemistry. John Wiley and Sons; 1990.
27. Devaquet A. Avoided Crossings in Photochemistry. Pure Appl Chem. 1975; 41:455–473.
28. Schwartz FP, Albrecht AC. One and Two-Photon Photochemistry in Rigid Solutions of Durene in 3-Methylpentane at 77 Degrees K. Chem Phys Lett. 1971; 9:163–165.
29. Simpson FB, Burris RH. Nitrogen Pressure of 50 Atmospheres Does Not Prevent Evolution of Hydrogen by Nitrogenase. Science. 1984; 224:1095–1097. [PubMed: 6585956]
30. Kubas GJ. Fundamentals of H_2 Binding and Reactivity on Transition Metals Underlying Hydrogenase Function and H_2 Production and Storage. Chem Rev. 2007; 107:4152–4205. [PubMed: 17927158]
31. Kubas GJ. Activation of Dihydrogen and Coordination of Molecular H_2 on Transition Metals. J Organomet Chem. 2014; 751:33–49.
32. Crabtree RH. Dihydrogen Complexation. Chem Rev. 2016; 116:8750–8769. [PubMed: 26974601]
33. Crabtree RH. Dihydrogen Binding in Hydrogenase and Nitrogenase. Inorg Chim A-Bioinor. 1986; 125:L7–L8.
34. Sweany RL. Photolysis of Hexacarbonylchromium in Hydrogen-Containing Matrices - Evidence of Simple Adducts of Molecular-Hydrogen. J Am Chem Soc. 1985; 107:2374–2379.
35. Sweany RL. Photolysis of (Cyclopentadienyl) Tricarbonylhydridometal and (Pentamethylcyclopentadienyl) Tricarbonylhydridometal Complexes of Tungsten and

Molybdenum in Dihydrogen-Containing Matrices - Evidence for Adducts of Molecular-Hydrogen. J Am Chem Soc. 1986; 108:6986–6991.

36. Loges B, Boddien A, Junge H, Noyes JR, Baumann W, Beller M. Hydrogen Generation: Catalytic Acceleration and Control by Light. Chem Commun. 2009:4185–4187.
37. Doherty MD, Grills DC, Huang KW, Muckerman JT, Polyansky DE, van Eldik R, Fujita E. Kinetics and Thermodynamics of Small Molecule Binding to Pincer-Pcp Rhodium(I) Complexes. Inorg Chem. 2013; 52:4160–4172. [PubMed: 23541116]
38. Phillips JC. Stretched Exponential Relaxation in Molecular and Electronic Glasses. Reports on Progress in Physics. 1996; 59:1133–1207.

Synopsis

N_2 reduction by nitrogenase involves the accumulation of four reducing equivalents at the active site FeMo-cofactor to form a state with two [Fe-H-Fe] bridging hydrides (denoted $E_4(4H)$, the Janus intermediate), which is activated to cleave the N≡N triple bond by the reductive elimination (*re*) of H_2. We report that photolysis of $E_4(4H)$ induces *re* of H_2 in two steps, each photoinduced. Results indicate the intermediate state in this process is an H_2 complex of FeMo-cofactor.

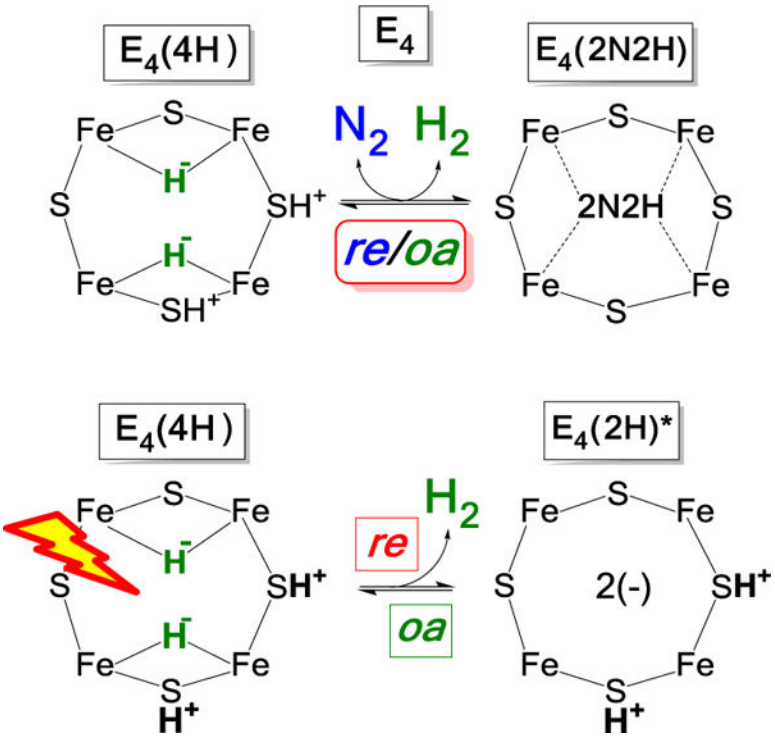

Figure 1.

Representations of the mechanistically central *re/oa* equilibrium that activates nitrogenase to break the N≡N triple bond (**upper**), and of the photoinduced *re/oa* equilibrium (**lower**). These cartoons represent the Fe 2,3,6,7 face of FeMo-co; but we emphasize they are not meant to be 'anatomically' precise.

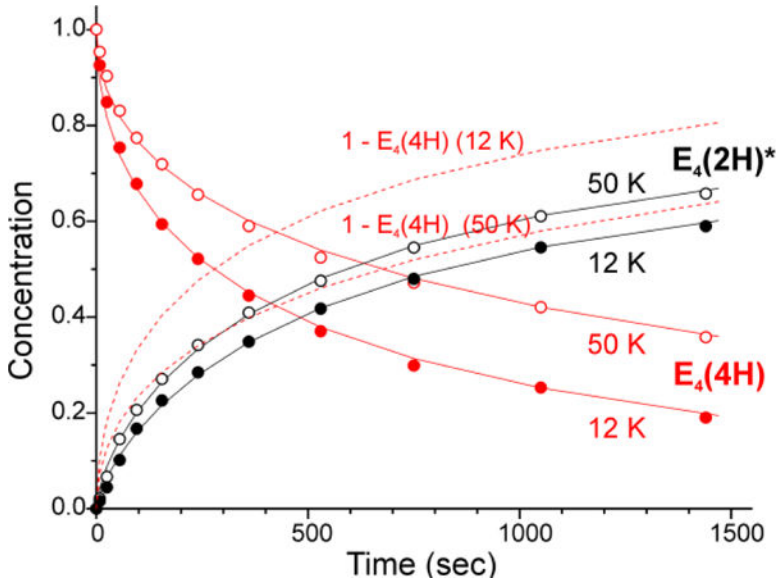

Figure 2.

Comparison of normalized 12 K and 50 K time courses of $E_4(4H)$ (red) and $E_4(2H)^*$ (black) states during irradiation of α-$70^{Val\rightarrow Ile}$ H_2O turnover sample with 450 nm laser diode light. Solid lines are to guide the eye; dotted lines show the lag in $E_4(2H)^*$ formation at 12 K.

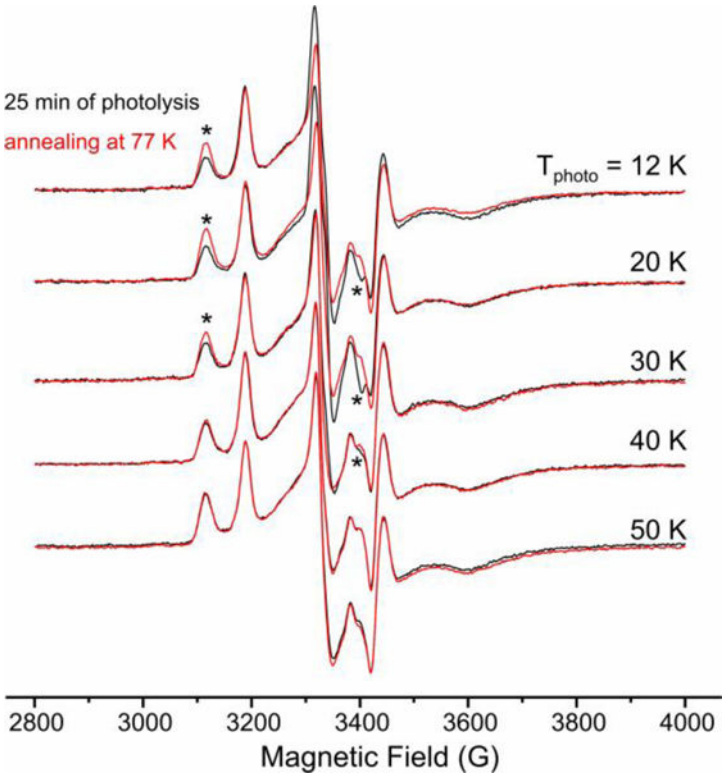

Figure 3.

Results of 77 K annealing of α-70$^{Val\rightarrow Ile}$ turnover irradiated at various temperatures. (*)-labeled features of EPR spectra indicate recovery of dihydride intermediate state E_4(4H) upon annealing (left) in parallel with disappearance of photoinduced species (right).

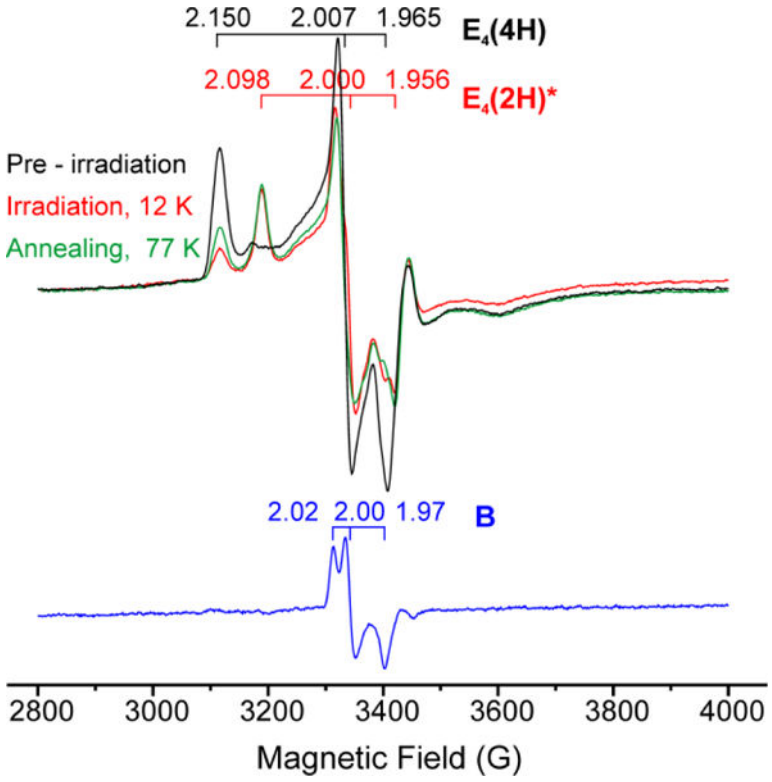

Figure 4.

Subtraction-elimination of E_4(4H) and E_4(2H)* signals from EPR spectrum of α-70$^{Val\rightarrow Ile}$ turnover irradiated at 12 K (red) with use of combination of spectra recorded before irradiation (black) and after 77 K annealing, which followed the irradiation (green). Result presents otherwise unresolved new photoinduced signal **B** (blue) unstable at 77K.

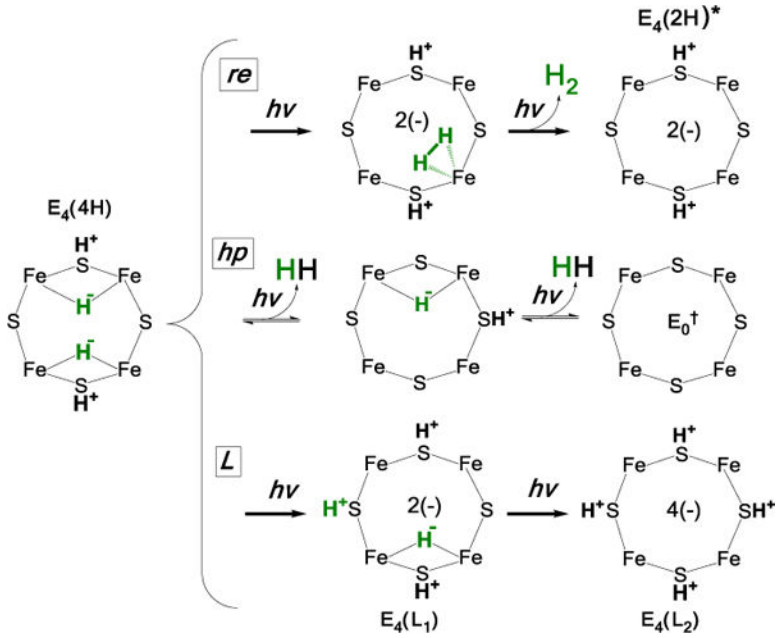

Fig 5. Alternative 2-step mechanisms for photoinduced reaction

(Top) *re*; assignment of intermediate discussed below; **(middle, bottom)** alternative mechanisms, see text.

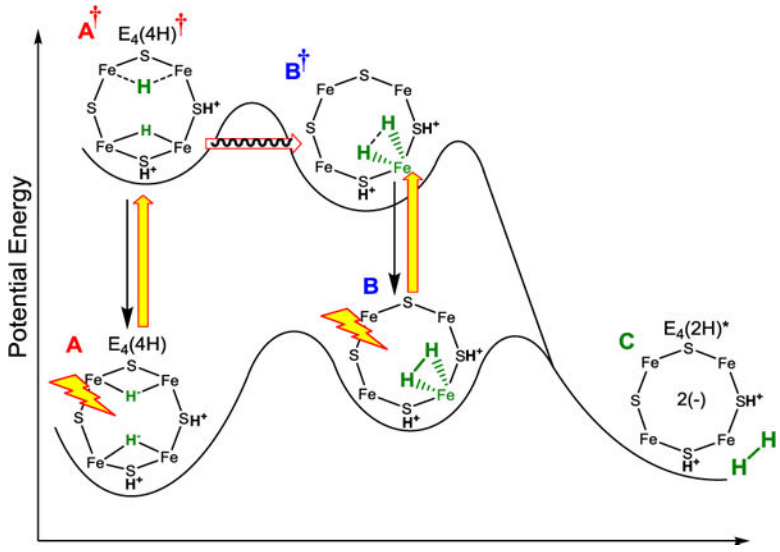

Figure 6.

Idealized energy landscape for the low-temperature photoinduced *re/oa* of the Janus intermediate, $E_4(4H)$. *Excited-state surface*: the proposed identifications of the states **A†**, **B**, and **B†** are discussed in the text. *Yellow arrows, photoexcitation; black arrows, relaxation, red* arrow, nuclear tunneling.

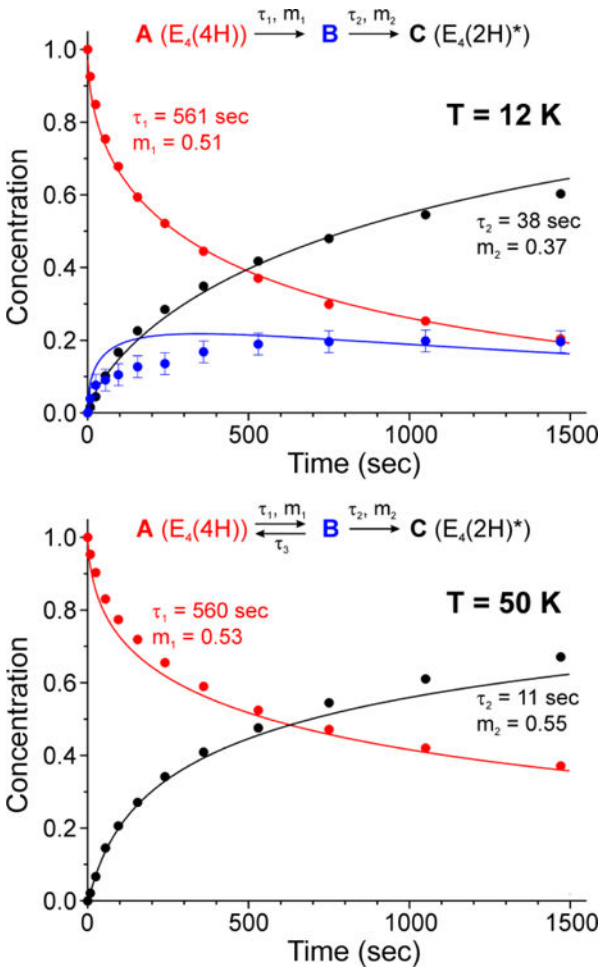

Figure 7.

Normalized time courses of $E_4(4H)$ (red) and $E_4(2H)^*$ (black) states measured during photolysis at 12 K (upper) and 50 K (lower) are shown fitted as previously described[7] in accordance with corresponding low and high temperature kinetic schemes. Data points for photoinduced intermediate **B** at 12 K were obtained with subtraction procedure described in Figs 4, S1, and are shown in comparison with the kinetic scheme prediction (blue trace). Low accumulation of **B** state at 50 K is due to back reaction step with time constant τ_3 = 160 sec.

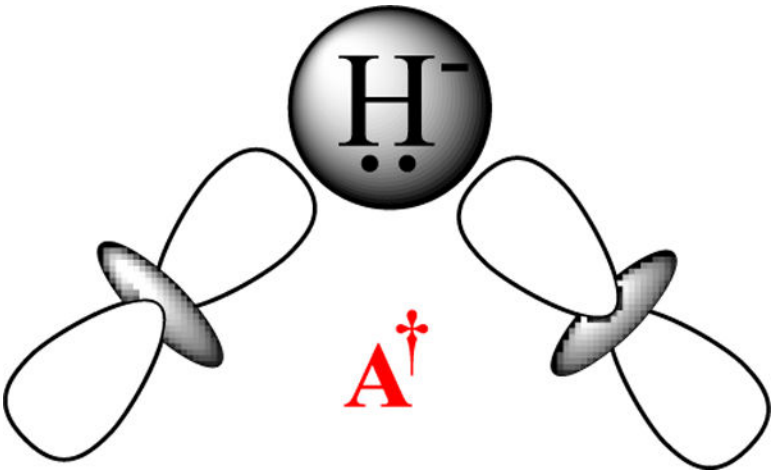

Figure 8.
Antibonding excited state of bridging hydride.

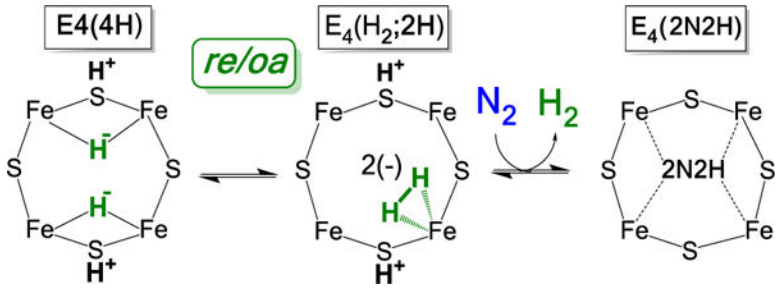

Figure 9.

Cartoon version of suggested catalytic pathway for *re/oa* activation of FeMo-co for N_2 reduction.

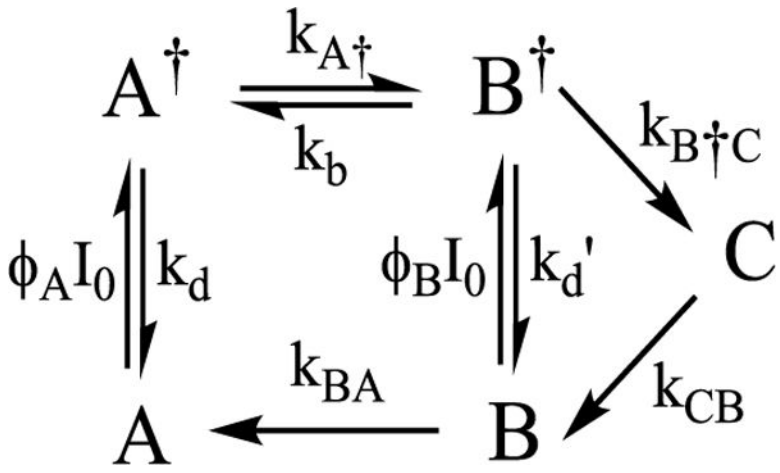

Scheme 1.

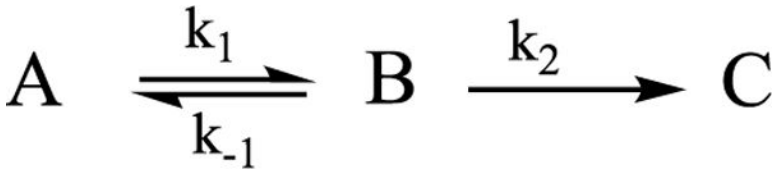

Scheme 2.